Correlation Between the Local SAR and Near *E* Field of the Dipole Antenna Close to the COST244 Phantom

Yoshio KOYANAGI, Koichi OGAWA*, and Koichi ITO**
Mobile Communications Company, Matsushita Communication Industrial Co., Ltd., Japan
/ Graduate School of Science & Technology, Chiba University, Japan
E-mail: koyanagi@pcd.mci.mei.co.jp
* Devices Development Center, Matsushita Electric Industrial Co., Ltd., Japan
** Department of Urban Environment Systems, Faculty of Engineering, Chiba University, Japan

1. INTRODUCTION

Because mobile phone terminals operate in proximity to the human body, biological effects by electromagnetic exposure have been investigated in several studies [1] – [3]. In the radio frequency (RF) range, the primary dosimetric parameter for the evaluation of the exposure is the specific absorption rate (SAR) [2]. The local SAR can be determined experimentally by measuring induced *E* field values caused in the tissue by absorption;

$$\mathrm{SAR} = \frac{\sigma E^2}{\rho} \ [\mathrm{W/kg}] \qquad (1)$$

where *E* is electrical field strength (RMS value) [V/m], σ is the conductivity[S/m] and ρ is the mass density [kg/m^3] of the lossy dielectric tissue. Since the compliance of the SAR limits is defined by the maximum SAR value at a specific place, it is important to expect SAR distribution exactly in the lossy medium.

In the vicinity of dipole-like sources, it has been reported by Kuster that there is a simple relation between the square of the incident *H* field strengths and the SAR distribution, SAR $\propto H^2$ [1]. But we usually estimate the SAR value by use of the internal *E* field data, like eq. (1), hence the relationship between fields inside and outside a medium with different properties is not well known. For example, the *E* field data of a half wavelength dipole antenna exist around the tip of the element, whereas the main SAR distribution exists around the feed point on the surface of the lossy medium, when antenna placed parallel to the antenna. Thus the behaviors of *E* field inner the boundary plane differ greatly from those of the outer side. The several papers have treated the behavior of the incident plane wave near the boundary plane of the lossy medium [4]. However, little has been investigated on the mechanism of that the incident *E* field is not related to the SAR distribution.

In this paper, the effect of the permittivity and the conductivity for the *E* field distribution inside and outside a medium has been investigated. To elucidate a general mechanism of SAR distribution, *E* field of a half wavelength dipole antenna close to the COST 244 phantom[5] at 2GHz has been analyzed using the FDTD method.

2. BOUNDARY OF THE LOSSY MEDIUM AND INCIDENT *E* FIELD

When plane waves propagate to *y* direction into a lossy medium, electromagnetic wave has been written in the followings;

$$\overline{E}(y,t) = \hat{z}_0 \sqrt{2} a e^{-\alpha y} \cos(\omega t - \beta y + \phi) \qquad (2)$$

$$\overline{H}(y,t) = \hat{x}_0 \sqrt{2} a x_0 e^{-\alpha y} \cos(\omega t - \beta y + \phi - \theta) \qquad (3)$$

$$\alpha = \omega \sqrt{\frac{\varepsilon' \mu}{2}} \left[\sqrt{1 + \frac{\sigma^2}{\omega^2 \varepsilon'^2}} - 1 \right]^{1/2} \qquad (4)$$

where $\theta = \arg(y_0)$, β is the phase constant, α is the attenuation constant[4], $\omega = 2\pi f$ and f is the frequency, σ is the conductivity, μ is the permeability and ε' is the real part of the permittivity of the medium.

By eq. (2)–(4), Ez and Hx components lose amplitude with increasing y according to the factor $e^{-\alpha y}$. When $\sigma / \omega\varepsilon' << 1$, attenuation constant α decreases when σ is large and ε' is small. The meaning of this term will be demonstrated that loss tangent ($\tan\delta = \sigma / \omega\varepsilon'$) decides the ratio of attenuation in the medium.

On the other hand, near E field distribution may change a lot at the boundary when a lossy medium is located close to the RF source. The reason will be explained that the near field data have any Ey component, in addition to the Ez component. Let us consider the interface between the free space and dielectric region 1. On the boundary of each region, electric field $\overline{E}_1$ and electric flux density $\overline{D}_1$ in the region 1 are continuous against the $\overline{E}_0$, $\overline{D}_0$ in free space, in the followings;

$$\hat{n} \times (\overline{E}_0 - \overline{E}_1) = 0 \tag{5}$$

$$\hat{n} \cdot (\overline{D}_1 - \overline{D}_0) = \hat{n} \cdot (\varepsilon_1 \overline{E}_1 - \varepsilon_0 \overline{E}_0) = \rho_s \tag{6}$$

where $\hat{n}$ is a unit of normal vector from the free space to the region 1, ε_0 and ε_1 are the complex permittivity in free space and the region 1, respectively. And ρ_s is the surface charge density, which may be assumed to be zero on the interface.

Eq. (5) and (6) show, the tangential component of E and the normal component of D against the boundary are continuous from the free space to the region 1. Now, we define the transmission coefficient τ from eq. (6) as the ratio of the normal component of the infiltration E_0 to incident E_1, in the followings;

$$\tau = \frac{E_{y1}}{E_{y0}} = \frac{|\varepsilon_0|}{|\varepsilon_1|} = \frac{\varepsilon_0}{\sqrt{\left(\varepsilon_0^2 \varepsilon_r^2 + {\sigma_1}^2 / \omega^2\right)}} \tag{7}$$

$$\varepsilon_1 = \varepsilon_1' - j\varepsilon_1'' = \varepsilon_r \varepsilon_0 - j\frac{\sigma_1}{\omega}, \quad \varepsilon_r = \frac{\mathrm{Re}[\varepsilon_1]}{\varepsilon_0}$$

Eq. (7) shows that, the incident normal component of E decreases in proportion to the difference in absolute values of the complex permittivity on the surface of the lossy medium.

3. CALCULATION MODEL

Figure 1 shows the analytical model of a half wavelength dipole antenna close to the COST244 phantom [5]. The phantom consists of a rectangular dielectric with the dimension of 200 mm x 200 mm x 200 mm. The dielectric properties are set to be homogeneous as $\varepsilon_r = 42.1$, $\sigma = 1.5$ S/m, $\rho = 1030$ kg/m^3 [6]. The half wavelength dipole antenna (0.49λ) at 2 GHz is placed both at a distance 10 mm from the phantom and with an orientation parallel to the body axis (z axis). The origin of coordinates is placed at the center of the phantom surface under the feed point of the antenna. The FDTD method has been employed to calculate the near field distribution. The size of the cells is $\Delta x = \Delta y = \Delta z = 2$ mm. The absorbing boundary condition is assumed on the Liao, and the time step is 3.85ps to satisfy the Courant stability condition.

In this paper the electric properties of the lossy medium have been varied like $\varepsilon_r = 1$–42.5, $\sigma = 0.1$–1.5 S/m to investigate the elucidate a general mechanism of changing E field distribution.

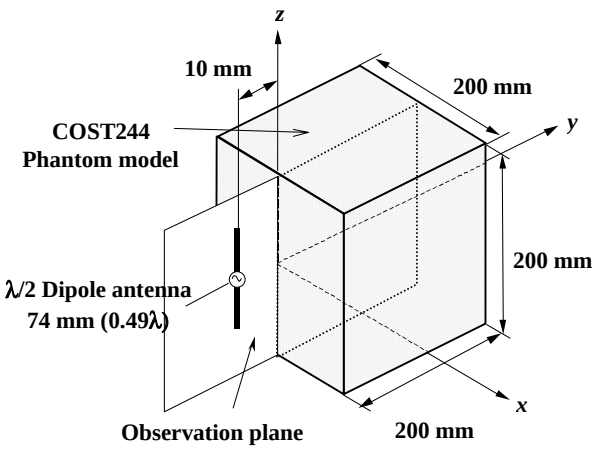

Fig. 1 FDTD calculation model.

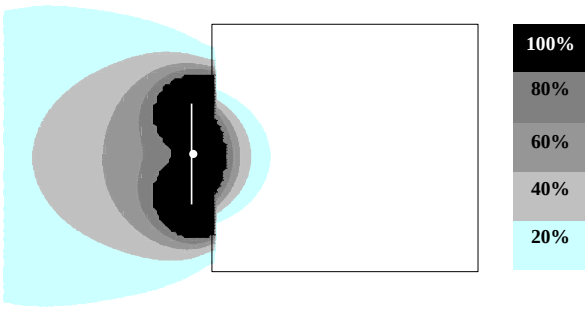

Fig. 2 *E*_Field data at *yz* plane.

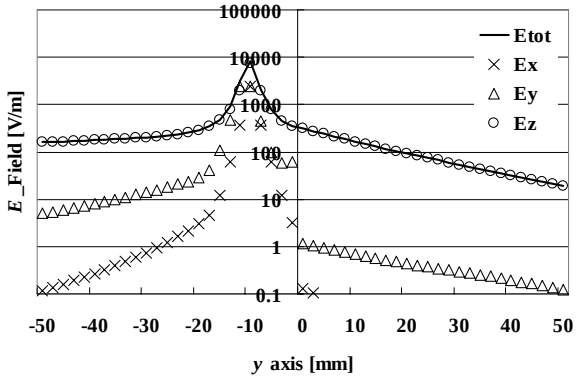

(a) *z* = -1 mm

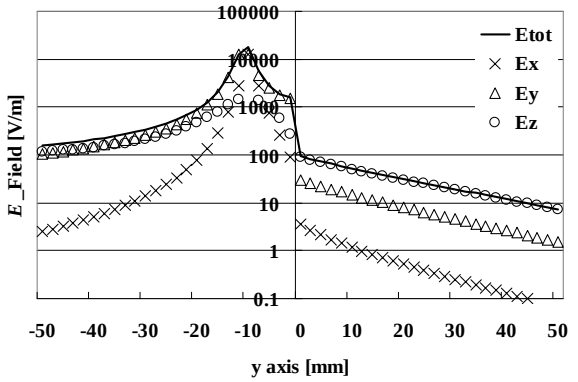

(b) *z* = -37 mm

Fig. 3 *E*_Field data on *y* axis.

4. RESULTS

Figure 2 shows the *E* field distribution at the *yz* plane (x = 0) when the antenna radiates 1W, and 100 % indicates E = 200 V/m. In Fig. 2, the main distributions are around the tip of the antenna element in free space. But into the phantom, the main *E* field distribution exists around the feed point. Therefore the tendencies differ greatly inner the boundary from the outer side of the phantom. Since the SAR value in the phantom will be estimated from the square of *E* field by eq. (1), the main SAR distribution exists around the feed point. Therefore, this distribution seems to have been caused by the incident *H* field.

Figure 3 shows the detail of *E* component of the Fig. 2 on the direction of y axis, z = –1 mm in (a) and z = –37 mm in (b). In Fig. 3, the right side of y = 0 shows the region in the phantom. Fig. 3 demonstrates that each *E* component decreases gradually in the loss medium according to the eq. (2) as gradient exp(-α). And the incident *E*y component dose not infiltrate into the phantom in comparison with *E*z component. Thus, it seems that the boundary plane is substantially existent particular for *E*y component. In the case of Fig. 3(b), although *E*y component is dominant outside the phantom, *E*z becomes dominant within the medium. In order to clarify these phenomenons, a theoretical investigation was made on a change of the permittivity and conductivity using the attenuation coefficient α in eq. (4) and the transmission coefficient τ in eq. (7).

Figure 4 shows the attenuation coefficient α of *E*z component in the medium at z = –37 mm. In Fig. 4, three lines show α values estimated by the *E*z component of FDTD analysis, and marker ○, △, ×, show theoretical values calculated by eq. (4). From this, α becomes small when σ is small and ε_r is large, that is easy to infiltrate. The estimated α value by the FDTD model as Fig. 1 and theoretical α value by eq. (4) agree well. The result clearly shows that the attenuation ratio of *E* field in the loss medium is decided mainly by the attenuation coefficient α, i.e. loss tangent (tanδ).

Figure 5 shows the transmission coefficient τ of *E*y component in the medium at z = –37 mm. In Fig. 5, three lines show τ values estimated by the ratio of the *E*y at boundary (y = 0) and incident *E*y in free space (y = –2 mm). And markers ○, △, ×, show theoretical τ values calculated by eq. (7).

From this, τ becomes small when σ or ε_r is large, i.e., both the real and imaginary part of the complex permittivity cause boundary loss. After all, the *E*y component orthogonal with a boundary plane hardly infiltrate into the lossy medium. In Fig. 5, estimated τ value by the FDTD model agrees well with theoretical τ value by eq. (7). This indicates that the infiltration ratio of *E*y field at the boundary of the lossy medium is decided mainly by the transmission coefficient τ. The above results have been confirmed that it is the same also at $z = -1$ mm on y axis.

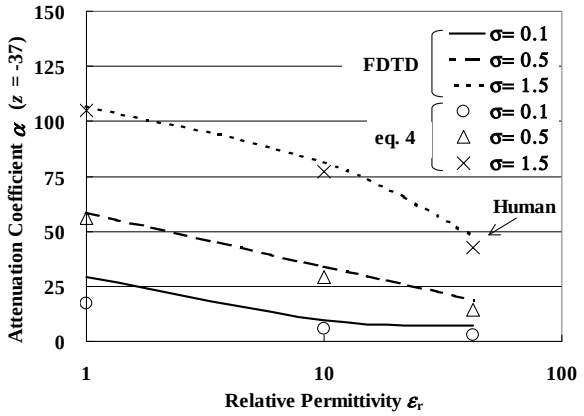

Fig. 4 Attenuation coefficient α of *E*z ($z = -37$).

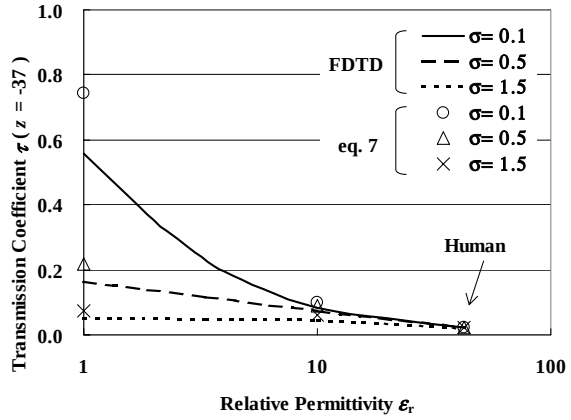

Fig. 5 Transmission coefficient τ of *E*y ($z = -37$).

In Fig. 4 and Fig. 5, the theoretical values at the human parameter indicated by the notes "Human" as $\varepsilon_r = 42.1$, $\sigma = 1.5$ S/m. The results were $\alpha = 42.8$ Np/m and $\tau = 0.02$. So in the case of the antenna close to the human body, incident *E*z component will not infiltrate into a deep region of the medium, due to suddenly decreases about 43 times compared with in free space. But this component becomes the main factor of SAR distribution near the surface. And incident normal component of *E* does not infiltrate into the medium due to a decrease to 2/100 at the boundary plane. Therefore, it seems that correlation between total incident *E* field and SAR distribution is expected to be sufficiently low.

5. CONCLUSION

The *E* field distributions of a dipole antenna close to a lossy medium, as a function of the ε_r and/or σ, have been investigated. *E* field distribution is formed by both the attenuation by loss tangent in the medium and the difference in absolute value of the complex permittivity, which cause a decrease in the normal component of incident *E* field. In the case of a half wavelength dipole antenna, tangential component of *E* against the boundary mainly exists near the feed point. It is for this reason that the main SAR distribution is formed around this area.

REFERENCES

[1] N. Kuster and Q. Balzano, "Energy absorption mechanism by biological bodies in the near field of dipole antennas above 300 MHz," IEEE Trans. Veh. Tech., vol. 41, no. 1, pp. 17-23, Feb. 1992.

[2] N. Kuster, Q. Balzano, and J. Lin, Mobile Communications Safety, London, U. K. Chapman & Hall, 1997.

[3] R. Y-S. Tay, Q. Balzano and N. Kuster, "Dipole configurations with strongly improved radiation efficiency for hand-held transceivers," IEEE Trans. A. P, vol. 46, no. 6, pp. 798-806, Jun. 1998.

[4] William H. Hayt Jr. and John A. Buck, " Engineering Electromagnetics / six edition," McGraw-Hill, 2001.

[5] COST244 WG3, "Proposal for numerical canonical models in mobile communications, " Proc. of COST244, pp. 1-7, Roma, Nov. 1994.

[6] C. Gabriel , " Complain of the dielectric properties of body tissues at RF and microwave frequencies, "Brooks Air Force Technical Report, AL/OE - TR - 1996 - 0037, 1996.